Nuclear Instruments and Methods in Physics Research B 266 (2008) 5050–5055

Contents lists available at ScienceDirect

Nuclear Instruments and Methods in Physics Research B

journal homepage: www.elsevier.com/locate/nimb

# Retrospective radon progeny measurements through measurements of $^{210}$Po activities on glass objects using stacked LR 115 detectors

C.W.Y. Yip, D. Nikezic, K.N. Yu *

*Department of Physics and Materials Science, City University of Hong Kong, Tat Chee Avenue, Kowloon Tong, Kowloon, Hong Kong*

ARTICLE INFO

*Article history:*
Received 26 April 2008
Received in revised form 23 August 2008
Available online 2 September 2008

*PACS:*
29.40
23.60

*Keywords:*
Radon
Radon progeny
$^{210}$Po
Implantation
Retrospective dosimetry
LR 115

ABSTRACT

A stacked LR 115 detector consisting of two active layers was proposed for determining $^{210}$Po activity in glass surfaces after deposition of short-lived radon progeny. The sensitivities of both active layers were calculated. Two glass samples were exposed in a chamber to determine the experimental calibration factors for the radon gas and progeny, which were then compared with the theoretical calibration factors from simulations. The experimental and the simulated calibration factors for radon progeny agreed well. The discrepancy between the calibration factors for radon gas was due to a much higher equilibrium factor used in the experimental calibration than the nominal value assumed in the simulation. A mini-survey of contemporary and retrospective radon progeny concentrations was carried out at 10 residential sites. A relationship between contemporary and retrospective radon progeny concentrations was not readily observable.



## 1. Introduction

It has been argued that case-control studies to estimate the risk of lung cancer due to radon exposure should preferably be based on long-term retrospective radon exposure assessments instead of contemporary radon exposure measurements [1–3] because of possible changes in exposures over time. Two methods of retrospective radon exposure assessment have been developed, namely, through surface traps (ST) and volume traps (VT). Both methods are based on determining the activity of $^{210}$Pb, (a long-lived $^{222}$Rn progeny with $T_{1/2}$ = 22.3 years) through measuring alpha particles emitted from its second successor $^{210}$Po, either in ST such as the surface of solid media (mostly glass) [4–11] or in VT such as the bulk of porous media (mostly furniture filling sponges) [12].

In this paper, we only focus on the ST method, in particular using glass surfaces. Atoms of short-lived $^{222}$Rn progeny, namely, $^{218}$Po, $^{214}$Pb, $^{214}$Bi and $^{214}$Po can accumulate and deposit on these surfaces. Due to the recoil after alpha decay of the $^{218}$Po and $^{214}$Po nuclides, some of the newly-formed atoms ($^{214}$Pb and $^{210}$Pb) can be incorporated into the surface. The activity of the long-lived $^{210}$Pb accumulated in a surface increases with the time of exposure. The ST method has been successfully applied in a number of previous surveys [3,13–16].

To determine the activity of $^{210}$Po implanted in the surface of a glass object, the "(CR–LR) difference technique" [10,11] is commonly used. Here, two solid-state nuclear track detectors (SSNTDs), namely, LR 115 and CR-39, were fixed side by side on the glass object under study. Since the CR-39 detector does not have an upper energy threshold, it can detect alpha particles emitted from the surface layer (originating from implanted $^{210}$Po) as well as from the volume of the glass object. The LR 115 detector has an upper energy threshold well below 5.3 MeV which is the energy of alpha particles emitted by $^{210}$Po (except for very thick removed layers during chemical etching) and it detects only alpha particles emitted from the volume. Therefore, the difference between the track densities on these two detectors (after correction for different sensitivities) can be used for measurements of $^{210}$Po implanted in the surface. The activity of $^{210}$Po (Bq m$^{-2}$) is given in [10,11] as

$$A_{^{210}\mathrm{Po}} = \frac{\mathrm{CR} - B \times \mathrm{LR}}{T \times K} \quad (1)$$

where CR is the net number of tracks per cm$^2$ on the CR-39 detector; LR is the net number of tracks per cm$^2$ on the LR 115 detector; $B$ is the ratio of track densities recorded on a CR-39 detector to that on an LR 115 detector attached to a piece of unexposed glass; $K$ is the sensitivity factor for the CR-39 detector to surface $^{210}$Po activity (in the unit tracks cm$^{-2}$ per Bq h m$^{-2}$) and $T$ is the period time (h) for which the CR-39 and LR 115 detectors are mounted on the glass surface.

* Corresponding author. Tel.: +852 27887812; fax: +852 27887830.
*E-mail address:* peter.yu@cityu.edu.hk (K.N. Yu).

0168-583X/$ - see front matter © 2008 Elsevier B.V. All rights reserved.
doi:10.1016/j.nimb.2008.08.010

A review of SSNTDs, including their use in retrospective radon dosimetry is given in [17]. The parameters $B$ and $K$ were determined in [18] for various removed layers from chemical etching for both the CR-39 and LR 115 detectors. Further studies have been carried out to relate the implanted $^{210}$Po activity to the exposure to radon progeny [19,20], and a preliminary survey of retrospective radon progeny measurements for dwellings based on implanted $^{210}$Po activities in glass objects has been carried out [21].

Although the (CR–LR) difference technique has become a default method for retrospective measurements of activities of $^{210}$Po implanted in the surface of glass objects, some simplifications or improvements of the methodology are possible. First, the involvement of two different types of SSNTDs is inevitably more tedious and introduces extra uncertainties. For example, the etching conditions of the two types of SSNTDs are very different. Moreover, as explained in [18], for the (CR–LR) difference technique, the response of the CR-39 and LR 115 detectors to different alpha particle emitters in the volume of the glass objects, as well as the response of the CR-39 detectors to $^{210}$Po on the surface of the glass objects should be determined, which relied on the availability of accurate $V$ functions of these detectors. The function $V$ is defined as the ratio between track etch rate $V_t$ and the bulk etch rate $V_b$, i.e., $V = V_t/V_b$. It is noted that $V$ functions are difficult to obtain and establish [22–25], and inevitably have uncertainties.

Secondly, for the (CR–LR) difference technique, the two SSNTDs are placed side by side on the glass surfaces and thus cover different positions. Although there were no detailed studies, the possibility of non-uniform background activities inside the glass objects cannot be ruled out. If such non-uniformity exists, applying separate detectors on two different positions on a glass object might lead to inaccurate results.

In the present work, a new method for determining the $^{210}$Po activities in glass surfaces is proposed. Instead of requiring an LR 115 detector and a CR-39 detector to be fixed side by side on the examined glass object, we use only one stacked LR 115 detector mounted against a single location on the examined glass object. By using the LR 115 detector alone, only the uncertainty in the $V$ function of this detector is relevant, which already reduces the total uncertainty of the method. Furthermore, now that only a single position of the glass surface is involved, the problem introduced by using two different positions is avoided.

## 2. Stacked LR 115 detectors and sensitivities of the active layers

The basic setup for a stacked LR 115 detector is shown in Fig. 1. Those used in the present studies (type 2, non-strippable) were purchased from DOSIRAD, France. They consist of a 12 μm red cellulose nitrate active layer and 100 μm clear polyester base substrate. In the present work, the stacked LR 115 detectors consist of two active layers. Active layer A is stripped from a piece of LR 115 detector with a thickness of 12 μm, and is placed in contact with the glass surfaces when in use. Active layer B is intact with its polyester base.

Active layer A registers only alpha particles emitted from the bulk glass volume. Due to the large energy of alpha particles emitted by $^{210}$Po and small implantation depth (<0.1 μm), active layer A will not register any alpha particles emitted from the surface implanted $^{210}$Po. Therefore, the response of active layer A can be written as

$$\rho_A = (\varepsilon_{A,V,U} C_U + \varepsilon_{A,V,T} C_T) t \quad (2)$$

where $\rho_A$ is the track density recorded on the active layer A (in track/m$^2$), $t$ is irradiation time (in s), $\varepsilon_{A,V,U}$ and $\varepsilon_{A,V,T}$ are the sensitivities of active layer A to alpha particles emitted in glass volume from the $^{238}$U radioactive decay series (U) and the $^{232}$Th decay series (T), respectively, both with the unit (track/m$^2$ s)/(Bq/kg), and $C_U$ and $C_T$ are the specific activities of $^{238}$U and $^{232}$Th in the glass (Bq/kg), respectively.

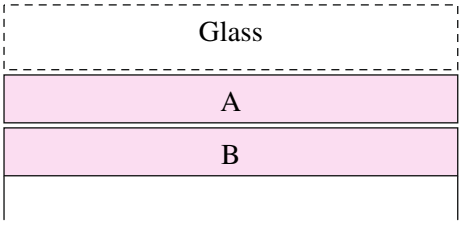


**Fig. 1.** Setup for a stacked LR 115 detector. Active layer A is stripped from a piece of LR 115 detector and will be placed in contact with the glass surfaces when in use. Active layer B is intact with its polyester base.

On the other hand, the active layer B registers alpha particles emitted from the bulk glass volume as well as alpha particles emitted from $^{210}$Po implanted in the glass surface. In this way, the response of the active layer B is

$$\rho_B = (\varepsilon_{B,V,U} C_U + \varepsilon_{B,V,T} C_T + \varepsilon_{B,S,Po} A_{Po}) t \quad (3)$$

where $\rho_B$ is the track density recorded on the active layer B, $\varepsilon_{B,V,U}$ and $\varepsilon_{B,V,T}$ are the sensitivities of the active layer B to alpha particles emitted in glass volume from the $^{238}$U decay series and the $^{232}$Th decay series, respectively, and $\varepsilon_{B,S,Po}$ is the sensitivity of the active layer B to alpha particles emitted by $^{210}$Po implanted into the surface, with the unit (tracks/m$^2$s)/(Bq/m$^2$), and $A_{Po}$ is the surface activity of $^{210}$Po (Bq/m$^2$).

Eqs. (2) and (3) have three unknown variables, namely, $C_U$, $C_T$ and $A_{Po}$. Strictly speaking, it is not possible to solve this system without additional information. Fortunately, the problem can be simplified if we know the relationship between $C_U$ and $C_T$. A number of different glass samples were measured using high-purity germanium spectrometry, and it was found that the ratio $C_U$:$C_T$ was relatively constant at about 6:4. Therefore, if we write $C_{tot} = C_U + C_T$ and $C_U = kC_{tot}$, $k = C_U/(C_U + C_T) \approx 0.6$. With the notations $\varepsilon_A = k \times \varepsilon_{A,V,U} + (1-k) \times \varepsilon_{A,V,T}$ and $\varepsilon_B = k \times \varepsilon_{B,V,U} + (1-k) \times \varepsilon_{B,V,T}$, we can express the activity of $^{210}$Po in the glass surface $A_{Po}$ as

$$A_{Po} = \frac{\rho_B}{\varepsilon_{B,S,Po} t} - \varepsilon_B \frac{\rho_A}{\varepsilon_A \varepsilon_{B,S,Po} t} \quad (4)$$

To determine the $^{210}$Po activity $A_{Po}$, two measurements are needed, i.e., the experimental track densities recorded on the active layers A and B, i.e., $\rho_A$ and $\rho_B$, respectively.

## 3. Theoretical determination of sensitivities of the active layers

The coefficients $\varepsilon_A$, $\varepsilon_B$ and $\varepsilon_{B,S,Po}$ in Eq. (4) are the sensitivities of the active layers of the LR 115 detectors, which can be derived if the $V$ function is known. Here we use our recently obtained $V$ function for the LR 115 detector:

$$V(R') = 1 + \left(A_1 e^{-A_2 R'} + A_3 e^{-A_4 R'}\right)\left(1 - e^{-R'}\right)$$

where $A_1 = 14.23$, $A_2 = 0.48$, $A_3 = 5.9$ and $A_4 = 0.0773$ [25], and $R'$ is the residual range of the alpha particles. The sensitivities were then determined using Monte Carlo methods. The ranges of alpha particles in glass were determined using the SRIM program [26], with "glass soda lime" having a density of 2.3 g cm$^3$ as the target. The energy loss and alpha particle spectra needed for Monte Carlo calculations are presented in Figs. 2 and 3. The energy loss of alpha particles in 12 μm of the LR 115 detector active layer is shown. Alpha particles with energies up to 2.6 MeV are absorbed within the sensitive layer and lose all their energy – the linear part corresponds to this situation. These particles do not reach the detector

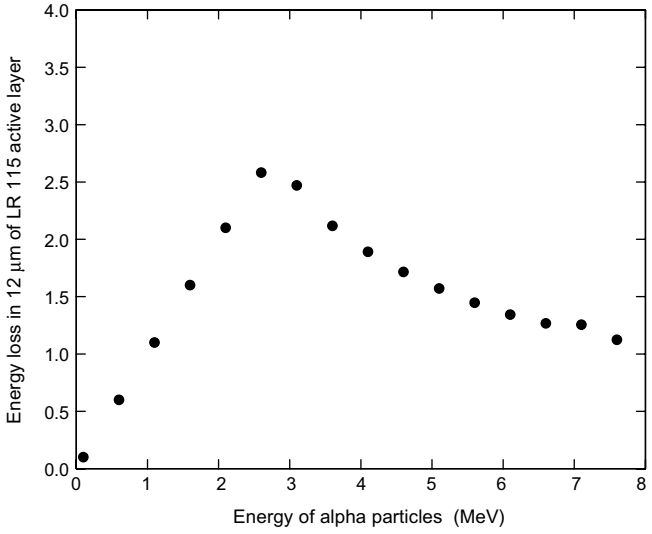


**Fig. 2.** Energy loss of alpha particles in 12 μm of the LR 115 detector active layer as a function of energy.

B. Alpha particles with larger energies lose a portion of their energies and reach detector B with a lower energy. In Fig. 3, the spectra of alpha particles incident on detectors A and B are presented. They are given in the terms of the probability density; $N(E)$ is the number of alpha particles which enter a detector with energies in the range $E$ to $(E + dE)$, and $N$ is the total number of alpha particles emitted in glass in the vicinity of the detector. The spectra are given separately for the $^{238}$U series and the $^{232}$Th series. The probability is smaller for alpha particles reaching the detector B than for those reaching the detector A.

The derived sensitivities for different removed layers during chemical etching of the active layers A and B are given in Tables 1–3. Since it was difficult to achieve exact removed layers as those shown in the tables, the actual sensitivities were determined from linear interpolation between the data.

## 4. Relationship between deposited $^{210}$Po activities measured by stacked LR 115 detectors and exposures to $^{222}$Rn and its progeny

Two glass samples were sent to the Health Protection Agency (HPA), Chilton, UK for exposure in their 43 $m^{-3}$ walk-in exposure chamber. The reference value of the integrated radon exposure and the equilibrium factor inside the exposure chamber (±1 sd) during exposure were provided by HPA as 100 ± 5 kBq $m^{-3}$ h and 0.680 ± 0.068, respectively. The total exposure to radon progeny concentration was thus 1.4 J s/$m^3$ (0.11 WLM).

After exposure, the glass samples were returned back to our laboratory for measurements using stacked LR 115 detectors. Two sets of detectors with a size of 3 × 3 $cm^2$ were mounted against each glass sample surface for about 160 d. The detectors were then etched in 10% aqueous solution of NaOH maintained at 60 °C by a water bath. Before etching, the stripped active layer A was replaced onto the original polyester base for easier manipulation. For the etching period, etching only from the top side of the active layer A was possible. The temperature was kept constant with an accuracy of ±1 °C and the etchant was stirred continuously using a magnetic stirrer (model no. SP72220-26, Barnstead/Thermolyne, Iowa, USA) to provide more uniform etching [27]. After etching for ~1 h, the detectors were removed from the etchant, rinsed with deionized water and dried. The removed thickness of the active layers during chemical etching was significantly affected by

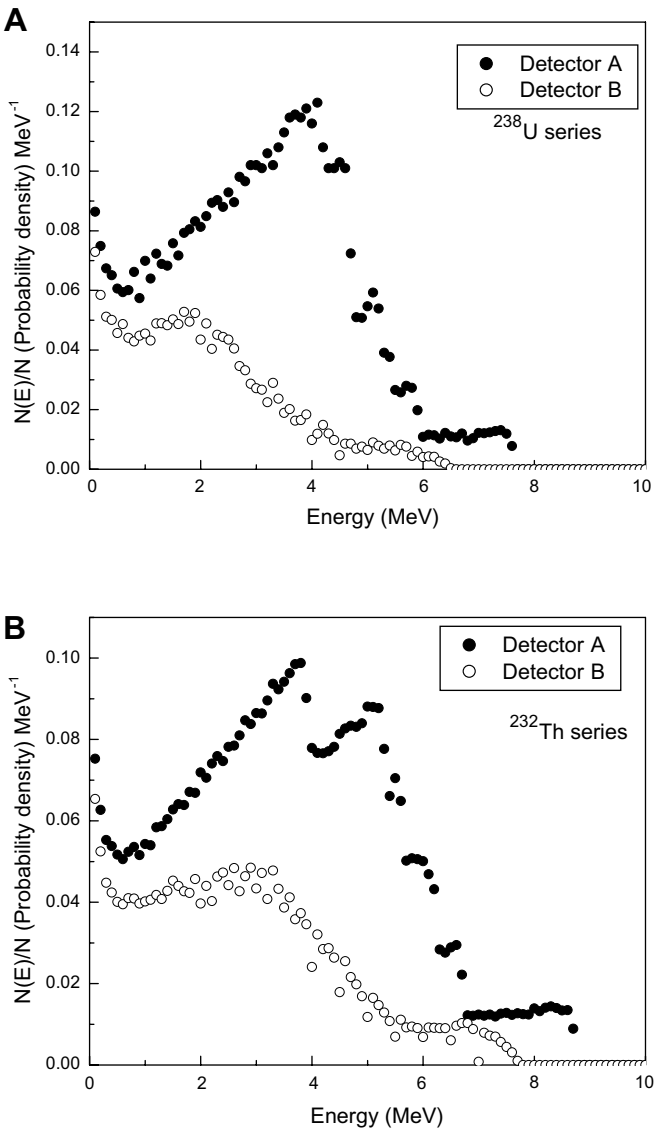


**Fig. 3.** Spectra of alpha particles incident on detectors A and B from the $^{238}$U series (upper panel) and the $^{232}$Th series (lower panel). The probability of an alpha particle with an energy $E$ entering the detector (A or B) is given as function of energy.

the presence and amount of stirring [27]. Surface profilometry [27] as well as infrared absorption [28] were adopted in the present work to measure the removed thickness of the active layers. The alpha particle tracks registered on the active layers were then counted under an optical microscope with 200× magnification. Only those tracks which completely perforated the active layers were counted. The track densities $\rho$ (number of tracks per unit area) were then found. The track densities, removed thickness and the exposed time of detectors on the glass surfaces are shown in Table 4.

**Table 1**
Sensitivity of active layer A to $^{238}$U and $^{232}$Th decay series (in $10^{-5}$ m) as a function of removed thickness (μm) of the active layer

| Removed thickness (μm) | $^{238}$U decay series | $^{232}$Th decay series |
|---|---|---|
| 4 | 0.491 | 0.390 |
| 5 | 0.991 | 0.778 |
| 6 | 1.535 | 1.203 |
| 7 | 2.056 | 1.662 |
| 8 | 2.555 | 2.143 |
| 9 | 3.035 | 2.639 |

**Table 2**
Sensitivity of active layer B to $^{238}$U and $^{232}$Th decay series (in $10^{-5}$ m) as a function of removed thickness (μm) of the active layer

| Removed thickness (μm) | $^{238}$U decay series | $^{232}$Th decay series |
|---|---|---|
| 4 | 0.304 | 0.329 |
| 5 | 0.512 | 0.610 |
| 6 | 0.716 | 0.888 |
| 7 | 0.921 | 1.150 |
| 8 | 1.145 | 1.339 |
| 9 | 1.388 | 1.629 |

**Table 3**
Sensitivity of active layer B to 5.3 MeV alpha particles from glass surface (track/m$^2$s)/(Bq/m$^2$)

| Removed thickness (μm) | $\varepsilon_{B,S,Po}$ |
|---|---|
| 4 | 0.124 |
| 5 | 0.158 |
| 6 | 0.179 |
| 7 | 0.200 |
| 8 | 0.223 |
| 9 | 0.247 |

**Table 4**
Experimental data for the stacked LR 115 detectors

| Glass sample | Active layer | Track density (track/cm$^2$) | Removed thickness (μm) | Mounting time on glass surface |
|---|---|---|---|---|
| 1 | A | 1419 | 5.41 | 153 d 19 h 10 min |
| | B | 1041 | 5.67 | |
| 1 | A | 1425 | 5.60 | 153 d 19 h |
| | B | 1141 | 7.80 | |
| 2 | A | 1501 | 6.40 | 160 d 4 h 25 min |
| | B | 814 | 6.20 | |
| 2 | A | 1260 | 5.18 | 160 d 4 h 30 min |
| | B | 929 | 5.35 | |

From the determined track densities, and through Eq. (4) and the associated coefficients $\varepsilon_A$, $\varepsilon_B$ and $\varepsilon_{B,S,Po}$ shown in Tables 1–3, and assuming $k = C_U/(C_U + C_T) = 0.6$, the activities of $^{210}$Po are calculated as shown in Table 5, which vary between 0.015 and 0.046 Bq/m$^2$, with a mean value of $A_{210_{Po}}$ (±1 sd) = 0.03 ± 0.01 Bq/m$^2$. If we assume the deposited activity of $^{210}$Po increases linearly with time, we can derive the experimental calibration factors $CF_g(exp)$ and $CF_p(exp)$ (with the subscripts g and p referring to exposures to radon gas and progeny, respectively) from the deposited activity $A_{210_{Po}}$. Using the total exposure to radon gas and radon progeny as 100 kBq h/m$^3$ and 1.4 J s/m$^3$, respectively, the calculated $CF_g(exp)$ varies between $0.042 \times 10^{-10}$ and $0.128 \times 10^{-10}$ Bq/m$^2$/(Bqs/m$^3$), and the calculated $CF_p(exp)$ varies between 0.136 and 0.418 Bq/m$^2$/WLM. Using $A_{210_{Po}} = 0.03 \pm 0.01$ Bq/m$^2$, the average $CF_g(exp)$ is about $(0.8 \pm 0.3) \times 10^{-10}$ Bq/m$^2$/(Bqs/m$^3$) and the average $CF_p(exp)$ is about 0.26 ± 0.12 Bq/m$^2$/WLM.

We have previously derived a theoretical calibration factor [20]. Here, all the parameters for the Jacobi model were changed simultaneously and randomly between the minimum and maximum values to obtain possible radon progeny concentrations for a chosen radon gas concentration. The equilibrium activities of radon progeny implanted in glass surfaces were then calculated. The relationships between the implanted activity and the concentrations of radon and its progeny then give the calibration factors. The calibration coefficient for the exposure of one year was obtained as 0.00086 (Bq/m$^2$)/(Bq/m$^3$). For short exposure periods, the amount of deposited $^{210}$Po increased almost linearly with time (see Figs. 7 and 9 in [20]). Therefore, the theoretical calibration factors from simulations can be evaluated as $CF_g(sim) = 0.27 \times 10^{-10}$ Bq/m$^2$/(Bqs/m$^3$) (with the subscript g again referring to exposures to radon gas). It can be seen that $CF_g(exp)/CF_g(sim) \approx 3$. If the "typical" equilibrium factor (from the Jacobi model) was 0.3, $CF_g(sim)$ can be transformed to $CF_p(sim) = 0.21$ Bq/m$^2$/WLM (with the subscript p again referring to exposures to radon progeny). We can observe that $CF_p(exp) \approx CF_p(sim)$. This result is particularly encouraging since this shows very good agreement between the calibration factor determined experimentally through measurements of $^{210}$Po activities on glass objects using the newly proposed stacked LR 115 detectors and that determined theoretically through computer simulations. The results that $CF_g(exp) \gg CF_g(sim)$ while $CF_p(exp) \approx CF_p(sim)$ also demonstrate the superiority of using $CF_p$ over $CF_g$. The discrepancy between $CF_g(exp)$ and $CF_g(sim)$ was due to a much higher equilibrium factor used in the experimental calibration than the nominal value assumed in the simulation. It is also remarked here that, for prolonged irradiation time, e.g., larger than 10 years, dependence of the implanted surface activity of $^{210}$Po per unit exposure on the exposure time starts to deviate from linear, and the actual values of $CF_g(sim)$ and $CF_p(sim)$ should be read from Figs. 7 and 9 in [20].

**Table 5**
Calculated $^{210}$Po surface activities (in Bq/m$^2$) with $k = C_U/(C_U + C_T) = 0.6$, and the experimental calibration factors $CF_g(exp)$ and $CF_p(exp)$ for exposures to radon gas and radon progeny, respectively

| Glass sample | $^{210}$Po activity (Bq/m$^2$) | $CF_g(exp)$ ($10^{-10}$ Bq/m$^2$/(Bq s/m$^3$)) | $CF_p(exp)$ (Bq/m$^2$/WLM) |
|---|---|---|---|
| 1 | 0.022 | 0.061 | 0.200 |
| 1 | 0.030 | 0.083 | 0.273 |
| 2 | 0.015 | 0.042 | 0.136 |
| 2 | 0.046 | 0.128 | 0.418 |

Another observation of the results shown in Table 5 is the non-uniform deposition of $^{210}$Po for glass sample 2, although the average value agrees with the two values obtained for glass sample 1. To take care of the possible non-uniform deposition of $^{210}$Po, in real life measurements, at least two stacked LR 115 detectors should be employed for each glass object and the mean value should be used.

## 5. Mini-survey of contemporary and retrospective radon progeny concentrations

A mini-survey was carried out at 10 different residential sites from February 2007 to February 2008. At each site, one to four glass objects, which range from mirrors, window panes, glass covering photos, glass on desks and/or cupboard glass, were examined using stacked LR 115 detectors. As mentioned before, to take care of the possible non-uniform deposition of $^{210}$Po, two stacked LR 115 detectors were employed for each glass object and the mean value was used. Due to technical problems, only one stacked LR 115 detector was recovered for the samples 2A, 2B, 2C and 4A. The exposure periods ranged from 2 to 6 months. Table 6 gives the derived $^{210}$Po activity on the glass surface (Bq/m$^2$) for the stacked LR 115 detectors. Non-uniform deposition of $^{210}$Po is readily observable from the data shown in Table 6.

At the same time the stacked LR 115 detectors were mounted against the examined glass objects, the contemporary long-term radon progeny concentrations were also surveyed using the "twins diffusion chamber" method [29,30] and the "proxy-equilibrium factor" method [31–33]. The proxy equilibrium factor $F_p$ was proposed [31,32] for passive monitoring of the equilibrium factor $F$ for short-lived $^{222}$Rn progeny.

The diffusion chambers employed for the present study were conical, with an inner base radius of 2.35 cm, top radius of 3.35 cm and height of 4.8 cm. To differentiate between the contributions

**Table 6**
Derived $^{210}$Po activity on the glass surface for the stacked LR 115 detectors

| Detector number | $^{210}$Po activity (Bq/m$^2$) |
|---|---|
| 1A-1 | 1.60 |
| 1A-2 | 5.80 |
| 1B-1 | 0.67 |
| 1B-2 | 2.44 |
| 1C-1 | 2.08 |
| 1C-2 | 4.00 |
| 2A-1 | 0.28 |
| 2B-1 | 0.35 |
| 2C-1 | 0.12 |
| 3A-1 | 1.31 |
| 3A-2 | 2.13 |
| 3B-1 | 0.53 |
| 3B-2 | 0.87 |
| 4A-1 | 0.99 |
| 4B-1 | 0.75 |
| 4B-2 | 0.59 |
| 4C-1 | 0.69 |
| 4C-2 | 1.28 |
| 5A-1 | 0.46 |
| 5A-2 | 0.10 |
| 6A-1 | 0.25 |
| 6A-2 | 0.32 |
| 7A-1 | 0.88 |
| 7A-2 | 1.02 |
| 7B-1 | 0.64 |
| 7B-2 | 0.24 |
| 8A-1 | 1.06 |
| 8A-2 | 0.53 |
| 8B-1 | 0.73 |
| 8B-2 | 1.02 |
| 8C-1 | 1.11 |
| 8C-2 | 0.69 |
| 9A-1 | 0.44 |
| 9A-2 | 0.49 |
| 9B-1 | 0.81 |
| 9B-2 | 0.64 |
| 9C-1 | 0.53 |
| 9C-2 | 0.43 |
| 9D-1 | 0.38 |
| 9D-2 | 0.82 |
| 10A-1 | 1.20 |
| 10A-2 | 1.13 |
| 10B-1 | 1.86 |
| 10B-2 | 1.84 |
| 10C-1 | 2.97 |
| 10C-2 | 3.07 |

Each sample number is expressed as (*x*Y-*n*), where *x* represents the site number (1–10), Y represents the object code at that site (A–D) and *n* represents the identification of the stacked LR 115 detector on the object (1 and 2).

from radon and thoron, two diffusion chambers were used, one for mainly recording the signal of radon while the other for (radon plus thoron). The difference between the signals recorded by the SSNTDs inside these two diffusion chambers can give the radon and thoron gas concentrations. At each site, two diffusion chambers were setup; one covered with filter paper and the other with an optimal thickness of polyethylene (PE) membranes to measure the radon and thoron gas concentrations [29]. An LR 115 SSNTD with a size of $3 \times 3$ cm$^2$ was attached to the center of the inner bottom of each diffusion chamber. In addition, one bare mode LR 115 detector, also with a size of $3 \times 3$ cm$^2$, was attached on the outside of the top lid of the diffusion chambers to determine $F_p$.

More recently, potential factors affecting measurements of $F$ using the $F_p$ method were studied in more detail [33]. The conclusions were (1) the removed active layer thickness of the LR 115 detector was a very critical parameter in determining $F_p$ and hence $F$; (2) the presence of thoron in the ambient environment would affect the track densities on the bare LR 115 detector but could be corrected for using the partial sensitivities to thoron; and (3) deposition of dust particles on the bare LR 115 detectors normally would not have significant effects.

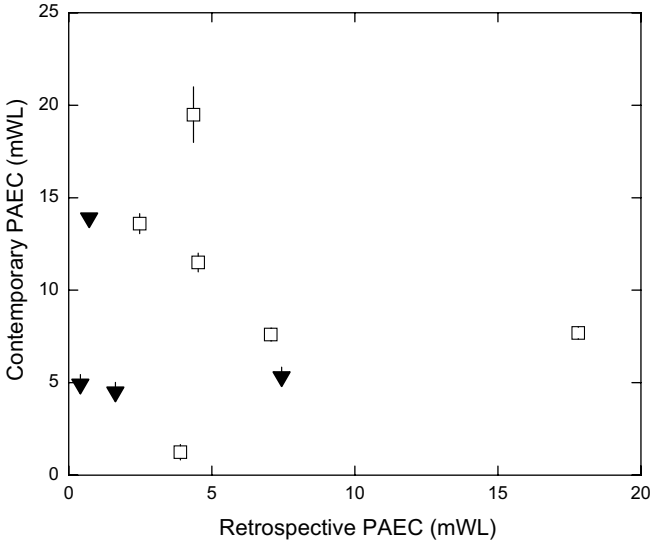


**Fig. 4.** Relationship between the contemporary PAEC determined using the $F_p$ method and the retrospective PAEC determined using stacked LR 115 detectors on glass objects. Solid triangles; measurements made when there were nearby construction/renovation sites. Open squares; measurements made when there were no nearby construction/renovation sites.

The relationship between the contemporary PAEC determined using the $F_p$ method and the retrospective PAEC determined using stacked LR 115 detectors on glass objects is shown in Fig. 4. From Fig. 4, a relationship is in fact not readily observable. Although this might be a result of the relatively small sample size, this nevertheless highlights the importance of long-term retrospective radon exposure assessments in case-control studies to estimate the risk of lung cancer due to radon exposure because of possible changes in the radon exposures over time. It is also noted that, out of the 10 surveyed residential sites, four were close to a construction site or renovation site when the measurements were made. For these sites, a larger-than-usual aerosol concentrations and thus larger contemporary (but not the retrospective) airborne radon progeny concentrations were expected [34,35].

## 6. Conclusions and discussion

A stacked LR 115 detector consisting of two active layers has been proposed here for determining $^{210}$Po activities in glass surfaces. This detector involves only one type of SSNTD and can be mounted at a single location on the examined glass object. From the track densities found on these two active layers, and through Eq. (4) and the associated coefficients the activities of $^{210}$Po can be calculated. The sensitivities are separately given for $^{238}$U and $^{232}$Th in Table 1. The sensitivities are not very different for the two series, and the largest discrepancy from the sensitivity obtained for $k = 0.6$ is smaller than 14%. In other words, the method described is not very sensitive to the actual ratio of $C_U/C_T$ in the examined objects.

Two glass samples were subjected to a total exposure of radon gas and radon progeny as 100 kBq h/m$^3$ and 1.4 J s/m$^3$. The experimental calibration factors $CF_g(exp)$ and $CF_p(exp)$ were compared with the theoretical calibration factors $CF_g(sim)$ and $CF_p(sim)$ from simulations. While $CF_g(exp) \gg CF_g(sim)$, $CF_p(exp) \approx CF_p(sim)$, which was due to a much higher equilibrium factor used in the experimental calibration than the nominal value assumed in the simulation. The result that $CF_p(exp) \approx CF_p(sim)$ is particularly encouraging since this shows very good agreement between experiments and computer simulations.

A mini-survey of contemporary and retrospective radon progeny concentrations was carried out at 10 different residential sites, using the "proxy-equilibrium factor" method and stacked LR 115 detectors on glass objects. A relationship between contemporary and retrospective radon progeny concentrations was not readily observable. Although this might be a result of the relatively small sample size, this nevertheless highlights the importance of long-term retrospective radon exposure assessments in case-control studies to estimate the risk of lung cancer due to radon exposure because of possible changes in the radon exposures over time.

## Acknowledgement

The present work was supported by a Research Grant CityU 123107 from the Research Grants Council of the HKSAR.

## References

[1] U. Bäverstam, G.A. Swedjemark, Radiat. Prot. Dosim. 36 (1991) 107.
[2] J.H. Lubin, J.D. Boice Jr., J.M. Samet, Radiat. Res. 144 (1995) 329.
[3] F. Bochicchio, J.P. McLaughlin, C. Walsh, Radiat. Meas. 36 (2003) 211.
[4] R.S. Lively, E.P. Ney, Health Phys. 52 (1987) 411.
[5] C. Samuelsson, Nature 334 (1988) 338.
[6] C. Samuelsson, L. Johansson, M. Wolff, Radiat. Prot. Dosim. 45 (1992) 73.
[7] R.S. Lively, D.J. Steck, Health Phys. 65 (1993) 485.
[8] J.A. Mahaffey, M.A. Parkhurst, A.C. James, F.T. Cross, M.C.R. Alavanja, J.D. Boice, S. Ezrine, P. Henderson, R.C. Brownson, Health Phys. 64 (1993) 381.
[9] C. Samuelsson, L. Johansson, Radiat. Prot. Dosim. 56 (1994) 123.
[10] R. Falk, L. Mellander, L. Nyblom, I. Ostergren, Environ. Int. 22 (Suppl.) (1996) S857.
[11] J.P. McLaughlin, Radiat. Prot. Dosim. 78 (1998) 1.
[12] S. Oberstedt, H. Vanmarcke, Health Phys. 70 (1996) 223.
[13] Z.S. Zunic, J.P. McLaughlin, C. Walsh, R. Benderac, Radiat. Meas. 31 (1999) 343.
[14] J. Paridaens, H. Vanmarcke, K. Jacobs, Z. Zunic, Appl. Radiat. Isot. 53 (2000) 361.
[15] A. Birovljev, R. Falk, C. Walsh, F. Bissolo, F. Trotti, J.P. McLaughlin, J. Paridaens, H. Vanmarcke, Sci. Total Environ. 272 (2001) 181.
[16] Z.S. Zunic, I.V. Yarmoshenko, K. Kelleher, J. Paridaens, J.P. McLaughlin, I. Celikovic, P. Ujic, A.D. Onischenko, S. Jovanovic, A. Demajo, A. Birovljev, F. Bochicchio, Sci. Total Environ. 387 (2007) 269.
[17] D. Nikezic, K.N. Yu, Mater. Sci. Eng. R 46 (2004) 51.
[18] D. Nikezic, C.W.Y. Yip, S.Y.Y. Leung, J.K.C. Leung, K.N. Yu, Nucl. Instrum. Methods A 568 (2006) 792.
[19] C. Walsh, J.P. McLaughlin, Sci. Total Environ. 272 (2001) 195.
[20] D. Nikezic, K.N. Yu, Radiat. Meas. 41 (2006) 101.
[21] C.W.Y. Yip, D. Nikezic, K.N. Yu, Radiat. Meas. 43 (Suppl. 1) (2008) S427.
[22] K.N. Yu, F.M.F. Ng, D. Nikezic, Radiat. Meas. 40 (2005) 380.
[23] C.W.Y. Yip, D. Nikezic, J.P.Y. Ho, K.N. Yu, Mater. Chem. Phys. 95 (2006) 307.
[24] S.Y.Y. Leung, D. Nikezic, J.K.C. Leung, K.N. Yu, Appl. Radiat. Isot. 65 (2007) 313.
[25] S.Y.Y. Leung, D. Nikezic, K.N. Yu, J. Environ. Radioact. 92 (2007) 55.
[26] J.F. Ziegler, J.P. Biersack, M.D. Ziegler, The stopping and range of ions in matter (2008), available at www.srim.org, originally based on TRIM code by J.F. Ziegler, J.P. Biersack, U. Littmark, The stopping and range of ions in solids, Pergamon Press, New York, 1985.
[27] C.W.Y. Yip, J.P.Y. Ho, V.S.Y. Koo, D. Nikezic, K.N. Yu, Radiat. Meas. 37 (2003) 197.
[28] F.M.F. Ng, C.W.Y. Yip, J.P.Y. Ho, D. Nikezic, K.N. Yu, Radiat. Meas. 38 (2004) 1.
[29] S.Y.Y. Leung, D. Nikezic, J.K.C. Leung, K.N. Yu, Nucl. Instrum. Methods B 263 (2007) 311.
[30] S.Y.Y. Leung, D. Nikezic, J.K.C. Leung, K.N. Yu, Nucl. Instrum. Methods B 263 (2007) 306.
[31] D. Nikezic, F.M.F. Ng, K.N. Yu, Appl. Radiat. Isot. 61 (2004) 1431.
[32] K.N. Yu, D. Nikezic, F.M.F. Ng, J.K.C. Leung, Radiat. Meas. 40 (2005) 560.
[33] K.N. Yu, S.Y.Y. Leung, D. Nikezic, J.K.C. Leung, Radiat. Meas. 43 (Suppl. 1) (2008) S357.
[34] K.N. Yu, E.C.M. Young, K.C. Li, Health Phys. 71 (1996) 179.
[35] K.N. Yu, T. Cheung, Z.J. Guan, E.C.M. Young, B.W.N. Mui, Y.Y. Wong, J. Environ. Radioact. 45 (1999) 291.